

FIXED TARGET BEAMS

V. Kain, H. Bartosik, S. Cettour-Cave, K. Cornelis, M. A. Fraser,
L. Gatignon, B. Goddard, F. Velotti, CERN, Geneva, Switzerland

Abstract

The CERN SPS (Super Proton Synchrotron) serves as LHC injector and provides beam for the North Area fixed target experiments. At low energy, the vertical acceptance becomes critical with high intensity large emittance fixed target beams. Optimizing the vertical available aperture is a key ingredient to optimize transmission and reduce activation around the ring. During the 2016 run a tool was developed to provide an automated local aperture scan around the entire ring.

The flux of particles slow extracted with the 1/3 integer resonance from the Super Proton Synchrotron at CERN should ideally be constant over the length of the extraction plateau, for optimum use of the beam by the fixed target experiments in the North Area. The extracted intensity is controlled in feed-forward correction of the horizontal tune via the main SPS quadrupoles. The Mains power supply noise at 50 Hz and harmonics is also corrected in feed-forward by small amplitude tune modulation at the respective frequencies with a dedicated additional quadrupole circuit. The characteristics of the SPS slow extracted spill in terms of macro structure and typical frequency content are shown. Other sources of perturbation were, however, also present in 2016 which frequently caused the spill quality to be much reduced.

INTRODUCTION

The Super Proton Synchrotron (SPS) at CERN delivers beam to the North Area fixed-target experiments using resonant slow extraction. It serves also as LHC injector and provides beam to the HIRADMAT [1] and AWAKE [2] facilities. The proton beams for fixed target physics are injected at a momentum of 14 GeV/c and need to cross transition in the early part of the acceleration to the 400 GeV/c extraction momentum. The requested intensities for fixed-target physics range from 3 to 4×10^{13} protons per cycle with typically 3300 cycles per day. Due to the high intensity and high duty cycle of the fixed-target beams, beam loss in the SPS has to be kept as low as possible to limit activation of the ring and maximising the acceptance of the machine is crucial.

The other challenge with fixed target beams in the SPS is to provide adequate spill quality for the North Area experiments. For an ideal slow extracted spill, the rate of extracted particles dN/dt should remain constant over the 4.8 s long extraction plateau. The spill is corrected in feed-forward by adjusting the tune directly through the main quadrupoles all around the SPS [3]. Also the fluctuations at 50 Hz and its harmonics are corrected in feed-forward. The servo-quadrupole system in long straight section 1 of the SPS is equipped with a 50, 100, 150 and 300 Hz current modulation of adjustable phase and amplitude for that purpose.

AUTOMATIC LOCAL APERTURE MEASUREMENT

The shape of the vacuum chambers follows the beam size variation around the ring circumference and the aperture with the flat vacuum chambers in the dipole magnets is optimised to accommodate the horizontal beam size during transition crossing and slow extraction. By design the acceptance in the vertical plane is smaller than in the horizontal plane. At low energy any further reduction of the vertical aperture due to orbit and misalignments directly translates into increased losses. The SPS vertical aperture bottleneck is expected to be at the TIDVG internal beam dump (vertical aperture of 42 mm).

The local aperture measurement tool

The automatic local aperture measurement tool is based on applying three-corrector-bumps at all quadrupole locations around the SPS. The bump amplitudes are increased linearly during the measurement period and the evolution of the beam intensity in the SPS is recorded. The amplitude is either increased from 0 mm to the maximum corresponding to the corrector circuit current limit or decreased from 0 mm to the minimum.

The mechanical aperture at a given location corresponds to the bump amplitude, where the intensity drops to zero as the entire beam is scraped off. A typical intensity evolution during a bump scan is plotted in Fig. 1. This method is independent of the transverse beam distribution, that can vary from shot to shot, but requires sufficient corrector strength.

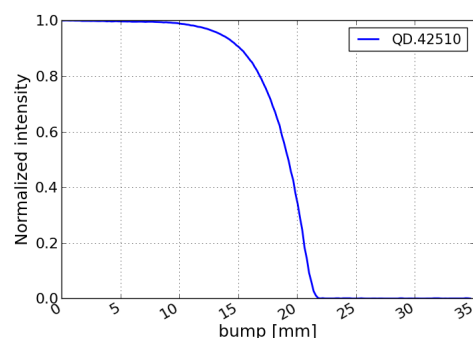


Figure 1: Intensity evolution during the scan of the amplitude of a three-corrector bump at location of QD.42510.

Limitations

The SPS orbit corrector magnets are limited to ± 3.5 A. For proton fixed-target beams, injected at 14 GeV/c and optics Q26, the maximum possible three-corrector-bump amplitude is thus ± 35 mm. This is sufficient for the vertical plane to

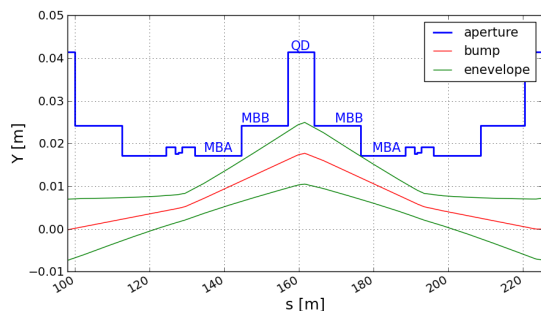


Figure 2: Mechanical aperture in the FODO cell of the SPS in the vertical plane with three-corrector bump and beam envelope. The bump will touch the aperture at the MBA to MBB or QD to MBB transition before reaching the QD aperture.

probe the mechanical aperture, but not for the horizontal one given the vacuum chamber dimensions.

The other limitation arises from the fact that the three-corrector-bumps span two SPS FODO cells and the mechanical aperture changes along a cell. In fact the bump as used during the scan does not probe the aperture of the defocusing quadrupole QD, but of the transitions from the QD to MBB main dipole vacuum chamber or from the MBB to MBA type of main dipoles as indicated in Fig. 2. In the current implementation of the tool the location of potential aperture bottlenecks that are found during the aperture scans cannot be better localised than to the region comprising the half cell upstream and downstream of the QD. The option to apply asymmetric bumps with four correctors to further localise the aperture restriction could be made available in an upgraded version of the local aperture measurement tool.

Results

The above introduced aperture measurement technique was developed, tested and finally deployed during the SPS run 2016. Low intensity $2 \mu\text{s}$ long MTE [4] beam of an intensity of $2 - 3 \times 10^{11}$ protons was used in a test cycle with a 3.6 s long 14 GeV/c plateau. The locations of all 108 defocussing quadrupoles of the SPS were scanned in positive and negative direction. Each scan was repeated 3 times for statistics. The error bars in the plots only contain the statistical errors.

The CERN accelerator control system provided all building blocks required for the automatic aperture scan. The YASP steering program [5] includes an automatic bump scan routine. YASP relies on the LHC software architecture (LSA) framework [6] which allows to configure knobs, i.e. bumps, to be applied in a user defined manner over time. An additional JAVA application had to be prepared to record the beam intensity measurement through the cycle and associate the data with the bump amplitude and the bump location name.

Two measurement series were carried out towards the end of the run in 2016, one on 18th of October and the second one on 22nd of November. The aperture was analysed as total aperture per location by combining the result of the positive and negative scan to be independent of the actual orbit on the test cycle. The total aperture measured at the different QD locations for the two scans is shown in the upper plot of Fig. 3. At the locations where no measurement point is indicated, the aperture was either never reached or the quality of the measurement was inadequate. In the long straight sections of every sextant, the QDs of half cells 17 and 19 are not neighboured by dipoles. Thus the aperture is larger than elsewhere and the correctors there are not strong enough to reach the mechanical aperture of the QD chamber itself. The exception is LSS1 where the SPS internal beam dump TIDVG is installed. The aperture at location QDA.11910 is much reduced because of it. Table 1 summarises the 4 locations found in the scans with the smallest vertical aperture around the ring.

As can be seen from the upper plot of Fig. 3, the aperture measurement is reproducible within typically better than 0.5 mm. Part of the measurement accuracy limitation comes from the noise on the BCT, which is in the order of $\approx 5 \times 10^8$ protons. The error bars in the plot do not indicate the error from the BCT resolution. More studies need to be carried out in 2017 to define the systematic error of the new measurement technique.

The consistency of the obtained results was cross-checked by scaling the obtained bump values at the QD locations to the locations of the MBB-to-MBA transitions as indicated in Fig. 2, where the beam loss should occur. Ideally the scaled values should be equal to the MBA aperture at this location. The aperture is however smaller than it should be at almost every location, see Fig. 3 (lower plot).

Table 1: The four locations with the smallest vertical aperture in the SPS in 2016.

location	aperture [mm]	error [mm]
QD.13310	43.1	± 0.5
QD.10710	43.3	± 0.2
QD.33110	44.6	± 0.6
QD.42310	45.2	± 0.7

The local aperture measurements suggest that the aperture bottleneck of the SPS is not at the beam dump, but at locations close to QD.10710 and QD.13310. Roughly 4 mm of aperture are missing at these locations. The total aperture measured at location QDA.11910 of 48.2 mm corresponds to ≈ 42.5 mm aperture at the center of the internal beam dump TIDVG, but 45.3 mm at the exit of the TIDVG, where the aperture bottle neck is supposed to be located. The theoretical aperture there is 42 mm. This inconsistency will have to be further investigated in 2017.

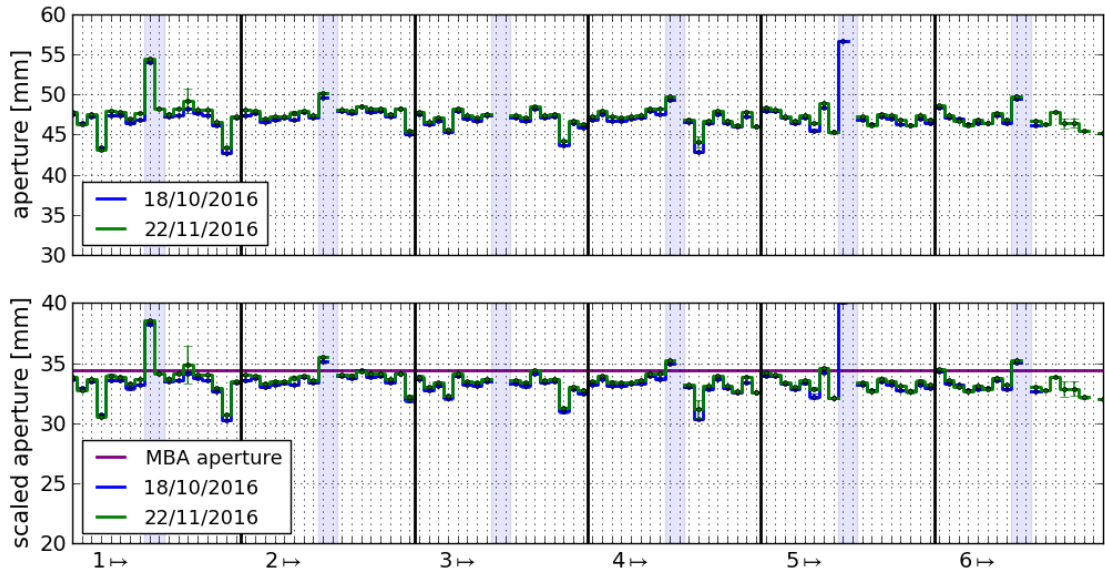


Figure 3: Total aperture measured at all defocusing quadrupole locations on 18th of October in blue and on 22nd of November in green. The numbers 1 - 6 on the bottom of the plot indicate the number of the corresponding sextant. The shaded areas correspond to the LSS. The lower plot shows the aperture measurements scaled to the location of the MBB-MBA transitions. The aperture of the MBA vacuum chamber is also indicated

SPILL QUALITY

The feed-forward based spill control was introduced in 2015 to remove the continuous trajectory changes on the North Area targets caused by the feedback controlled slow extraction [3]. The feed-forward is calculated only upon request. On a shot-by-shot basis, the spill quality relies on the reproducibility of the machine.

The hysteresis of the SPS magnets is not sufficiently modelled in the SPS control system. Any changes to the set of magnetic cycles played one after the other, the so-called super-cycle, have an impact on the beam parameters and hence on the flux of extracted particles during slow extraction. A measure of the uniformity of the spill is the "effective spill length" [7] which is defined as:

$$t_{efs} = \frac{[\int_{t_1}^{t_2} f(t) dt]^2}{\int_{t_1}^{t_2} [f(t)]^2 dt} \quad (1)$$

where $f(t)$ is the extracted intensity as a function of time. Fig. 4 and 5 show the evolution of the circulating intensity and extracted intensity calculated from the decay of the intensity during the extraction flat-top. The extracted intensity ramp-up at the beginning of the spill is introduced on purpose as the RF structure takes roughly ≈ 500 ms to diminish to an acceptable level for the North area experiments. Any events during this time are not taken into account. The situation in

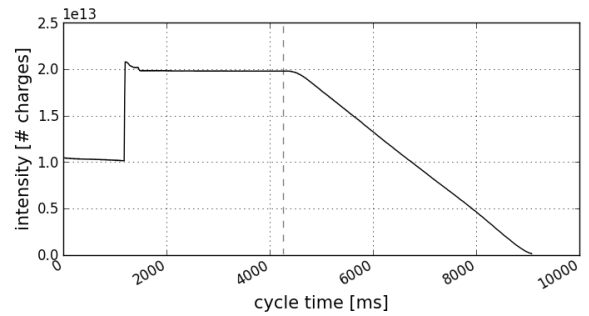


Figure 4: Evolution of the intensity through the fixed target cycle in the SPS in 2016. The dashed line indicates the moment at which the slow extraction starts.

Fig. 4 corresponds to a well adjusted spill and the effective spill length calculated according to (1) is $t_{efs} \approx 4500$ ms. If LHC 450 GeV/c cycles are added to the super-cycle or the dynamic economy mode is enabled, where the cycles are not fully played in case no beam is injected, the beam parameters will change. The effect on the extracted intensity before running the feed-forward algorithm is shown in Fig. 6 and 7. The effective spill length is reduced to 3800 ms for that case.

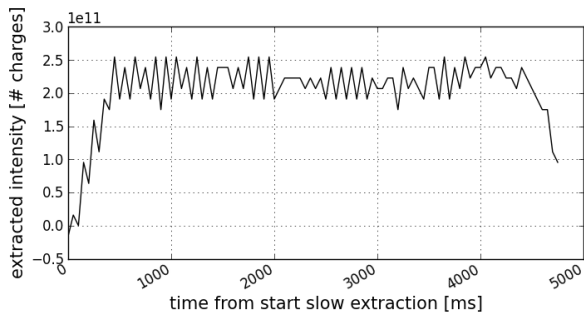


Figure 5: Extracted intensity as function of time on the extraction plateau of the fixed target cycle calculated from the intensity evolution in Fig. 4.

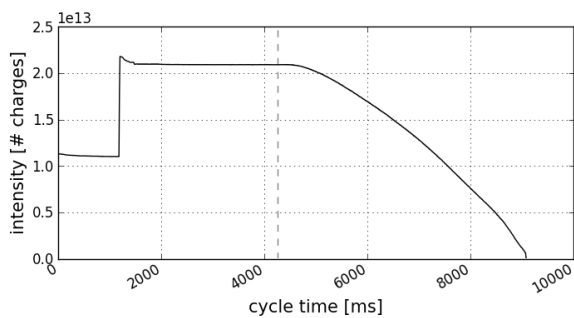


Figure 6: Evolution of the intensity through the fixed target cycle in the SPS in 2016 after a super cycle change. The dashed line indicates the moment at which the slow extraction starts. The beam is not extracted with a constant rate.

2016 Effective spill length

The typical value of the effective spill length for the 10.8 s long fixed target cycle in the SPS with a 4800 ms flat-top was ≈ 4500 ms. Due to hysteresis reasons, as explained above, the expected spill length could however be much reduced for extended periods. Fig. 8 shows the evolution of the effective spill length during 24 h where the LHC was in machine development (MD) and LHC beam had to be provided frequently by the SPS leading to many super-cycle changes. Whereas the first few hours of Fig. 8 are representative for a so-called production super-cycle with high duty cycle for the North Area, the period of the first shaded

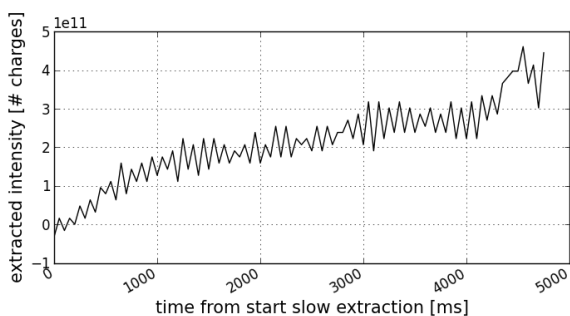


Figure 7: Extracted intensity as function of time on the extraction plateau of the fixed target cycle calculated from

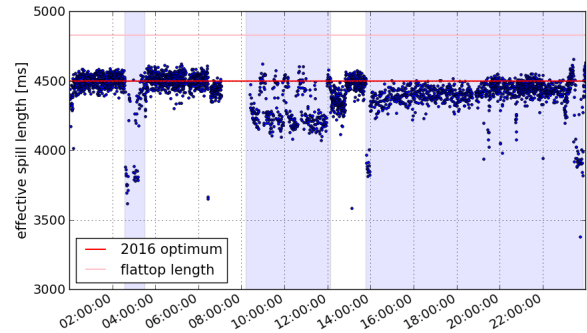


Figure 8: Evolution of the effective spill length during 24 h on 6th of October 2016. The shaded areas indicate times where LHC beam production cycles were in the SPS super-cycle. The first periods included LHC cycles with beam dedicated to the LHC with the LHC not continuously requesting beam such that the dynamic economy was played. During the last extended period a setting-up cycle for LHC beam was in the super-cycle with constant beam request.

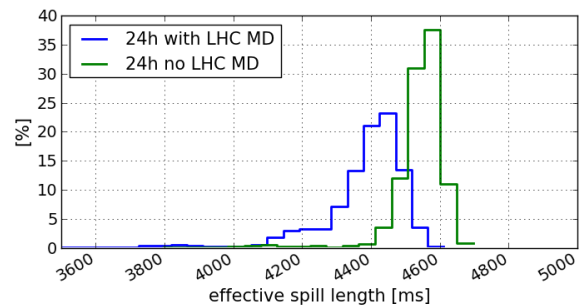


Figure 9: Distribution of effective spill length over 24 h on 6th of October, 2016, with MD in the LHC and 24 h on 16th of October, 2016, without MD in the LHC.

area is typical for an LHC filling super-cycle in terms of effective spill length. Fig. 9 shows the comparison of the distribution of effective spill lengths over 24 h with LHC MD (6th of October 2016) and a typical day with the occasional LHC filling or infrequent super-cycle changes in the SPS (16th of October 2016). Not surprisingly, the more stable running period without LHC MD leads to a narrower effective spill length distribution and also a slightly higher average effective spill length.

The hysteresis of the main dipoles seems to be the main cause of the spill macro structure variations with super-cycle changes [8]. In 2017 online field measurements of the reference magnets will be available. It is hoped that the analysis of this data will allow to build an automated correction algorithm.

Spill frequency content

As was discussed in [3] the SPS slow extracted spill is strongly modulated at 50 Hz and its harmonics. Without active correction the intensity fluctuations can be as high as 100 %. The amplitude and phase of the 50 Hz and higher

FIXED TARGET BEAMS

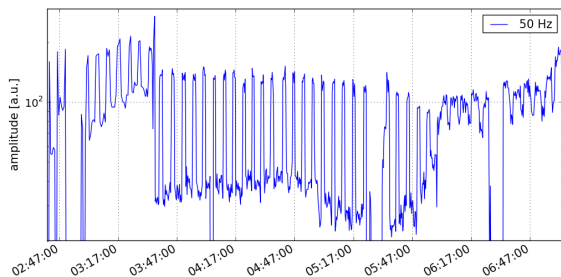


Figure 10: Evolution of the amplitude of the 50 Hz content in the spill. The 50 Hz amplitude bursts occur every few minutes.

harmonics modulations drift over time and the correction has to be frequently adjusted. In 2016 the system used to feed forward a small amplitude compensating tune modulation was calibrated for its spill phase response. As a result of this campaign a deterministic automatic algorithm could be put in place to adjust the modulation parameters. The adequate amplitude of the modulation is derived from an automatic scan.

Despite the more performant tools, the 50 Hz spill ripple seemed to be uncorrectable at times. Recording the evolution of the 50 Hz amplitude without changing the correction revealed the cause of this issue. The amplitude of the 50 Hz ripple does not slowly drift over time, but its amplitude is increased by up to a factor 5 for a short period of a few minutes and then decreased again. These bursts re-occur with a period of several minutes. Fig. 10 shows an example of such an observation. The bursts are not always present. For the time being no correlation with any modes of operation could be established.

Another problem in 2016 was the fact that strong modulation of the extracted intensity did not only occur at 50 Hz and higher harmonics thereof, but also at about 30 Hz or 65 Hz. The amplitudes of the peaks at these frequencies could be as high as of the 50 Hz lines, Fig. 11, but no active correction is available at these frequencies. The origin of these disturbances need to be found and corrected at the source. The FFT of the current of the QF main quadrupole circuit in the SPS also showed ≈ 30 Hz in the spectrum when the disturbance was strong on the spill, see Fig. 12. When the quadrupole power supply was swapped towards the end of the run in 2016, the 30 Hz issue disappeared.

SUMMARY & CONCLUSION

Optimising the vertical acceptance in the SPS is fundamental for minimising losses with high intensity fixed-target beams at low energy. An automated tool for measuring the local aperture at all defocusing quadrupoles was developed and tested in 2016. The results show that the vertical aperture bottleneck of the SPS is not at the internal beam dump TIDVG, but in the vicinity of QD.13310 and QD.10710. Also in sextant 3 and 4 bottlenecks were found.

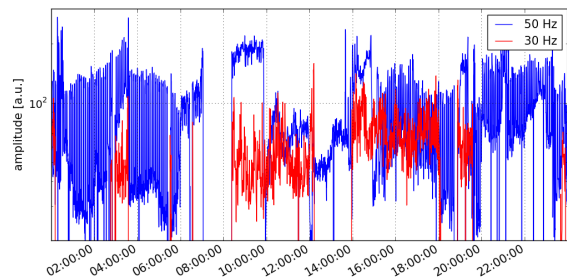


Figure 11: Evolution of the amplitude of the 50 Hz and 30 Hz content in the spill on 6th of October 2016. 50 Hz bursts are also present during most of the time of the observation time.

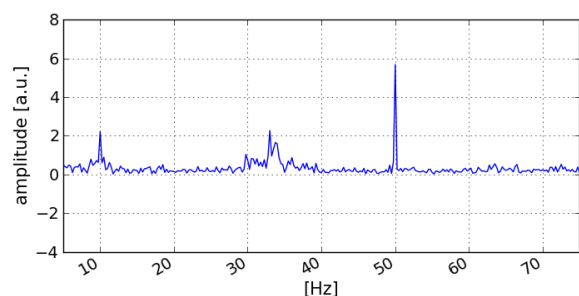


Figure 12: FFT of the current of the QF circuit during the slow extraction plateau on 6th of October 2016. Lines with large amplitude at 50 Hz as well as around 30 Hz can be seen in the spectrum.

The SPS slow extracted spill can be well corrected with feed-forward algorithms controlling the rate of extracted intensity as well as the 50 Hz and higher harmonics spill ripple. Good spill quality on a shot-by-shot basis relies however on reproducibility and several effects lead to that neither the spill macro structure nor the harmonic content of the spill were stable. Uncompensated hysteresis effects of the main field might be the origin of the macro structure changes. Work is underway to understand and model the hysteresis better and make it part of automated correction algorithms. Noise in the spill at 30 and 65 Hz is most probably induced by the main power supplies. Swapping the QF power supply already removed the 30 Hz ripple. More performant tools are now available to correct the 50 Hz and harmonics modulation of the spill. To really profit from these tools though, the origin of the 50 Hz bursts will have to be found and removed.

REFERENCES

- [1] N. A. Tahir et al., *New J. Phys.* 10, 073028 (2008)
- [2] E. Gschwendtner, et al., "Feasibility Study of the Awake Facility at CERN", IPAC, Shanghai, China, 2013
- [3] V. Kain et al., "New spill control for the slow extraction in the multi-cycling SPS", IPAC2016, Busan, North Korea.
- [4] M. Giovannozzi, et al., "Operational Performance of the CERN Injector Complex with Transversely Split Beams", *Phys. Rev. Accel. Beams* 20, 014001 (2017)
- [5] J. Wenninger, "YASP: Yet Another Steering Program"
- [6] D. Jacquet et al., "LSA - The High Level Application Software of the LHC and its Performance during the first 3 years of Operation", ICALEPCS, San Francisco, USA, 2013.
- [7] H. Weisberg, "Effective spill length monitor", AGS division technical note, Brookhaven National Laboratory, New York, 1980.
- [8] F. Velotti et al., "Investigation of the remanent field of the SPS main dipoles and possible solutions for machine operation", these proceedings.